ELSEVIER

Journal of Chromatography A, 955 (2002) 35–52

JOURNAL OF CHROMATOGRAPHY A

www.elsevier.com/locate/chroma

Measurement and modeling of the equilibrium behavior of the Tröger's base enantiomers on an amylose-based chiral stationary phase

K. Mihlbachler[a,b,c], K. Kaczmarski[a,d], A. Seidel-Morgenstern[c], G. Guiochon[a,b,*]

[a]*Department of Chemistry, University of Tennessee, Knoxville, TN 37996-1600, USA*
[b]*Division of Chemical and Analytical Sciences, Oak Ridge National Laboratory, Oak Ridge, TN 37831-6120, USA*
[c]*Department of Chemical Engineering, O.-v.-Guericke University Magdeburg, Magdeburg, Germany*
[d]*Rzeszòw University of Technology, Rzeszòw, Poland*

Received 5 December 2001; received in revised form 1 March 2002; accepted 1 March 2002

Abstract

The binary isotherms of the two enantiomers of Tröger's base were measured on a system made of pure 2-propanol as the mobile phase and of Chiralpak AD, a chiral stationary phase (CSP) based on amylose tri-(3,5-dimethylphenyl carbamate). The experimental data were acquired using both frontal analysis and the perturbation method. The results obtained are most unusual. The adsorption of the more-retained (−)-enantiomer is not competitive: the amount adsorbed onto the CSP at equilibrium with a constant concentration of the (−)-enantiomer is independent of the concentration of the (+) enantiomer. On the other hand, the adsorption of the less-retained enantiomer is cooperative: the amount of this (+)-enantiomer adsorbed by the CSP at equilibrium with a constant concentration of this enantiomer increases with increasing concentration of the (−)-enantiomer. Such a phenomenon has hardly ever been reported. A model equation is proposed that accounts well for all these isotherm data. © 2002 Elsevier Science B.V. All rights reserved.

Keywords: Enantiomer separation; Chiral stationary phases, LC; Adsorption isotherm; Multilayer adsorption; Equilibrium-dispersive model; Tröger's base

1. Introduction

Due to the FDA position on the use of enantiomers in the manufacturing of pharmaceuticals [1], there is now a considerable interest in the pharmaceutical and fine chemicals industries for the preparation of highly pure enantiomers. The direct approach, the use of an appropriate enantioselective synthesis, is often expensive and difficult to develop. It is inconvenient in the discovery phase and in phase I trials. The use of separation processes that can separate rapidly and economically the two enantiomers and/or purify one of them is then most useful. Even at the production level, a hybrid approach, combining a partially enantioselective synthesis and an enantioseparation is often the one making the most economical sense. The need to develop economical implementations of available separation processes and to achieve a high product purity requires the use of sophisticated methods that allow the

*Corresponding author. Tel.: +1-865-974-0733; fax: +1-865-974-2667.
E-mail address: guiochon@utk.edu (G. Guiochon).

0021-9673/02/$ – see front matter © 2002 Elsevier Science B.V. All rights reserved.
PII: S0021-9673(02)00228-5

proper estimate of the optimum values of the design and operation parameters of a preparative separation. Computer-assisted method development is now developing rapidly in the various modes of chromatography. This approach is particularly useful for simulated moving bed separations (SMB), in which case empirical optimization is slow and most costly.

Because preparative chromatographic processes are based on the difference between the equilibrium behaviors of the feed components in the selected phase system, the determination of accurate estimates of the competitive equilibrium isotherms of the main components of the mixture to separate is the first step in the computer assisted optimization of these processes. Knowledge of the isotherm behavior often contributes to explain the retention mechanism and may help to suggest approaches to improve the separation, hence the production rate. This is of particular interest for enantioseparations.

Several static and dynamic methods have been described for the determination of the equilibrium isotherms of pure compounds and of the competitive isotherms of binary or more complex mixtures [2–4]. The essential principle of these methods consists in measuring the concentration or amount of the compounds studied in the stationary phase at equilibrium with a solution of known composition used as the mobile phase. In static methods, the amount adsorbed on the CSP at equilibrium is weighed, directly or indirectly, and the operation is repeated at increasing solution concentrations. If accurate, these methods, however, are slow and consume large amounts of precious chemicals. Because mass transfers between phases are necessarily rather fast in chromatographic systems (otherwise they would not be used), dynamic methods are preferred.

For single component isotherms, the dynamic methods were first introduced by Glueckauf [5]. They are faster and need lesser amounts of chemicals than static methods. The most practical and popular dynamic method is frontal analysis (FA) [2]. It relates the point of the isotherm at a certain mobile phase concentration to the elution time of the breakthrough curve of the solution at this concentration. The perturbation method (PM) [2,6,7] or elution on a plateau [2] relates the slope of the isotherm at a certain concentration and the retention time of a small perturbation of this concentration. Since the achievement of the equilibrium between the stationary and mobile phases of known concentration is a prerequisite, the FA and PM methods can be easily combined. Although widely used, the elution by characteristic points method (ECP), which derives the isotherm from an integral of the diffuse side of the elution profile of a large sample, is less useful because it assumes the column to have an infinite efficiency and, accordingly, introduces a model error in the determination of isotherm data, an error that is significant when using columns of moderate efficiency [8]. For competitive isotherm determinations, both the FA and PM methods can be used. However, they both become significantly more complex to implement [2].

The aim of this paper is to illustrate how the unusual peculiarities of the adsorption behavior of a pair of enantiomers on a CSP may sometimes influence the selection of the most appropriate method for the determination of the equilibrium isotherms of the two feed components. We show also how the modeling of such data may require the use of sophisticated adsorption models. Nevertheless, even in such a difficult case, the band profiles calculated using the isotherm model so derived are in excellent agreement with the experimental data, suggesting that our classical approach remains valid and that computer-assisted optimization is more than ever a realistic possibility.

2. Theory

2.1. Chromatographic models

The accurate modeling of a separation process requires (1) a set of mass conservation equations; (2) appropriate initial and boundary conditions that describe the exact process implemented; (3) the binary (in the case of a racemic mixture) equilibrium isotherms; and (4) a suitable model of the mass transfer kinetics. The simplest mass conservation equation is the mass balance of the equilibrium dispersive model. This model assumes that there is constant equilibrium of the feed components between the two phases of the chromatographic system and that the finite efficiency of the column used can be accounted for by an additional contribution to the

axial dispersion. This model should be preferred to more complex ones whenever the mass transfer kinetics is sufficiently fast (or when the rate controlling factor is a diffusion, as it seems to be in the separation studied here [9]. As we show later, in agreement with previous results obtained with Tröger's base [9], this model works well in the present study.

2.1.1. Equilibrium dispersive mass balance

The mass balance of this model for compound i is written [2]:

$$\frac{\partial C_i}{\partial t} + u\frac{\partial C_i}{\partial z} - D_{ap}\frac{\partial^2 C_i}{\partial z^2} + \frac{\partial q_i}{\partial t} = 0 \quad (1)$$

where q and C are the stationary and mobile phase concentrations of component i, respectively, t is the time, z the distance along the column, $F = (1-\varepsilon)/\varepsilon$ is the phase ratio, with ε the column total porosity, u is the mobile phase velocity, and D_{ap} the axial dispersion coefficient. To simplify calculations, we assumed that the axial dispersion coefficient is the same for both enantiomers. This coefficient is related to the column efficiency at infinite dilution through [2]:

$$D_{ap} = \frac{uL_c}{2N} \quad (2)$$

where L_c is the column length and N its efficiency (i.e. the number of theoretical plates). Note that the mobile phase velocity is a function of the column external or interparticular porosity.

In the case discussed here, we need two equations like Eq. (1), one written for each of the two enantiomers. The concentrations q_i and C_i in these two equations are related through the set of binary isotherms (see later). This system of equations has no algebraic solutions but is conveniently solved numerically, using the backward forward finite difference method [10]. To ensure numerical stability of these calculations, the spatial increment is determined as a function of the linear velocity and the column efficiency [11]. The accuracy of the solutions calculated with this algorithm has been demonstrated previously [2,6,12,13].

2.1.2. Initial and boundary conditions

The solution of a system of partial differential equations requires a set of appropriate initial and boundary conditions. This set of conditions describes in mathematical terms the experiment that is actually carried out. In elution, the initial state of the column is its equilibrium with a stream of the pure mobile phase, hence, the initial condition is

$$C(0, z) = 0 \quad (3)$$

The typical boundary condition in elution is the injection of a rectangular pulse of feed solution, with

$$\begin{aligned} C(0, 0) &= C_{feed} \quad 0 \le t \le t_p \\ C(0, 0) &= 0 \quad t > 0 \text{ or } t > t_p \end{aligned} \quad (4)$$

where t_p and C_{feed} are the duration and feed concentration, respectively.

2.2. Models of adsorption equilibrium isotherms

These models relate the composition of the two phases at equilibrium. Linear models are valid only under the experimental conditions used in analytical chromatography, at low concentrations. To achieve economical productions rates, however, preparative chromatography must be conducted at high concentrations. Under such conditions, the isotherms are rarely linear. For mixtures, the amount of a compound adsorbed at equilibrium depends usually not only on its own concentration in the solution but also on the composition of the entire solution. In almost all known cases, multicomponent isotherms are competitive, i.e. the amount of one compound adsorbed in equilibrium with a constant concentration of this compound decreases with increasing concentrations of the other feed components [2].

Statistical thermodynamics [14,15] shows that binary isotherms are given by the following general equation:

$$q_i = \frac{q_s C_i P'(C_1, C_2)}{P(C_1, C_2)} \quad (5)$$

where $P(C_1, C_2)$ is a polynomial of degree n and $P'(C_1, C_2)$ is its first partial derivative. The Langmuir isotherm model corresponds to the polynomial of the first degree:

$$q_i = \frac{q_s b_i C_i}{1 + \sum_{l=1}^{M} b_l C_l} \quad (6)$$

In spite of its simplicity, this model accounts well for an important fraction of experimental results. The quadratic isotherm:

$$q_1 = \frac{q_s C_1 (b_1 + b_{12} C_2 + 2 b_{11} C_1)}{1 + b_1 C_1 + b_2 C_2 + b_{12} C_1 C_2 + b_{11} C_1^2 + b_{22} C_2^2} \quad (7)$$

$$q_2 = \frac{q_s C_2 (b_2 + b_{12} C_1 + 2 b_{22} C_2)}{1 + b_1 C_1 + b_2 C_2 + b_{12} C_1 C_2 + b_{11} C_1^2 + b_{22} C_2^2} \quad (8)$$

corresponds to the polynomial, $P(C_1, C_2)$, of the second degree [2,16]. With the proper set of numerical values, this isotherm may exhibit an inflection point [17,18]. This general form also includes the bilangmuir isotherm model [2], often used to account for the adsorption behavior of enantiomers on certain CSP. Depending on the numerical values of the different parameters in Eqs. (7) and (8), a wide variety of different isotherms can be obtained. This model could not, however, account for the kind of cooperative rather than competitive isotherm behavior that we encountered with the Tröger's base enantiomers.

The unusual adsorption behavior observed in this study can be interpreted by a multilayer adsorption isotherm model that is also based on statistical thermodynamics [14,15]. Assuming the formation of three layers on the active sites of the packing leads to a third order polynomial [see Eq. (5)]. A common saturation capacity q_s for both enantiomers is chosen for this model. Only one equilibrium parameter of the third layer K_{d211} shows significant influence on the adsorption isotherm. This parameter describes the adsorption of the less-retained compound onto agglomerate of the two enantiomers previously adsorbed. More detailed explanation about this model can be found elsewhere [19]. For the less-retained enantiomer the equation of the isotherm model is defined as following:

$$q_1 = q_s \frac{K_1 C_1 (1 + 2K_{d1} C_1 + K_{d12} C_2) + K_2 C_2 (K_{d21} C_1 + 2K_{d211} K_{d21} C_1^2)}{D}$$

$$q_2 = q_s \frac{K_2 C_2 (1 + 2K_{d2} C_2 + K_{d21} C_1 + K_{d211} K_{d21} C_1^2) + K_1 C_2 K_{d21} C_1}{D}$$

where

$$D = 1 + K_1 C_1 + K_2 C_2 + K_1 K_{d1} C_1^2 + K_2 K_{d2} C_2^2 + (K_2 K_{d21} + K_1 K_{d12}) C_1 C_2 + K_2 K_{d21} K_{d211} C_1^2 C_2 \quad (9)$$

Note a slightly different nomenclature is used to characterize the adsorption behavior (e.g. K_i equivalent to b_i, $K_i K_{di} = b_{ii}$, and $K_i K_{dij} = b_{ij}$).

As an alternative, a more empirical adsorption isotherm model is introduced that accounts for the unique cooperative adsorption behavior of the less-retained enantiomer and for the S-shaped adsorption isotherm of the more-retained enantiomer. The isotherm model of the less-retained enantiomer [see Eq. (10)] assumes a relatively high degree of adsorbate–adsorbate association. The more-retained enantiomer is model by the quadratic isotherm Eq. (8).

$$q_1 = \frac{b_a C_1 (q_{max} - k_2 C_2)}{1 + b_a C_1} + \frac{k_2 b_b C_1 C_2}{1 + b_b C_1} \quad (10)$$

This isotherm model proposed two different binding sites for the less-retained compound on the surface of the CSP with a maximum saturation capacity q_{max}. However, this enantiomer when pure can interact only with the binding sites of the first type. Then, in the absence of the more-retained enantiomer, the isotherm model reduces to a Langmuir isotherm (first term in Eq. (10)). When both enantiomers are present in a mixture, however, the sites of the second type are occupied by the more-retained enantiomer and an association between the CSP and molecules of both enantiomers is formed. Therefore, the adsorption of the less-retained enantiomer has a higher saturation capacity in the presence of the second enantiomer than without it. The distribution between these two sites is strongly dependent on the concentration of the two compounds. Their population is low at low concentration of more-retained enantiomer. Therefore, the binary adsorption behavior of the less-retained enantiomer becomes cooperative instead of being competitive as it usually is.

Because an association between molecules of the less-retained enantiomer takes place on the sites of the second type, the isotherm of the more-retained

enantiomer has an inflection point that the model accounts for. This model could (but in its form used here later does not) take into account a possible influence of the less-retained enantiomer on the adsorption of the more-retained one. Experimental results suggest that, if there is competition or cooperation for the more-retained enantiomer, its contribution is too small to be significant. Detailed information regarding the agreement between this isotherm model and experimental data are given later (see Section 4.1.2).

2.3. Methods of determination of equilibrium isotherms

The two most practical methods for the accurate determination of binary equilibrium isotherms are frontal analysis and the perturbation method. In this study, we used both methods for reasons that will become clear later.

2.3.1. Frontal analysis

FA is the most commonly used method of isotherm determination because of its accuracy and its relative simplicity. For single component isotherms, a series of data points is directly derived from the integrals of successive breakthrough curves of solutions of increasing concentrations [2]. This integral is proportional to the amount of solute adsorbed in the stationary phase at equilibrium with the corresponding solution. For multicomponent isotherms, breakthrough curves can also be used, but with some restrictions [20]. The breakthrough curve of a binary mixture has two waves separated by an intermediate plateau. If the initial condition for a breakthrough curve is that the column is in equilibrium with a finite concentration of the feed, the elution times of these two waves depend on these initial concentrations. Thus, it is necessary either to determine the composition of the solution eluting from the column during the intermediate plateau or to adopt as initial condition the equilibrium with the pure mobile phase, in which case only the pure less-retained component is eluted during the intermediate plateau. Usually, its concentration is the same or higher (in the case of displacement) as the one in the mobile phase used. However, the method is more difficult to implement and less accurate when the isotherm is convex downward, i.e. antilangmuirian, since in this case the front of the elution profile is diffuse and its rear self-sharpening. However, self-sharpening rear fronts are usually less steep than self-sharpening front. Furthermore, the data are difficult to measure in a relatively wide concentration range surrounding that corresponding to the inflection point of the isotherm. As we show later, this is the situation that we encountered with the more-retained enantiomer studied in this work.

2.3.2. Perturbation method

The PM method is extremely simple, since it merely requires analytical-size injections on successive concentration plateaus of increasing concentrations [5,7,21,22]. These injections can be of either a vacancy (i.e. of a sample of the pure mobile phase) or of a solution differing in composition from that of the plateau. Such an injection perturbs the equilibrium between the two phases and causes in the case of racemic mixtures two perturbations that migrate along the column. The retention times of these perturbations are recorded. It is easily shown [2,7] that the retention volumes of these perturbations are given by

$$V_{r,i}(C_1,\ldots,C_n) = V_0\left(1+\frac{1-\varepsilon}{\varepsilon}\frac{dq_i}{dC_i}\right) \quad i = 1,\ldots,n \tag{11}$$

where dq_i/dC_i is the total derivative the isotherm, itself given by

$$\frac{dq_i}{dc_i} = \sum_{j=1}^{N}\frac{\partial q_i}{\partial c_j}\cdot\frac{dC_j}{dC_i} \quad i = 1,\ldots,n \tag{12}$$

For single component isotherms, the total derivative is the conventional derivative. So, these isotherms are easily obtained by simple integration of the dependence of the retention volume of the perturbations as a function of the plateau concentration, solving Eq. (11) for q. For binary isotherms, however, this is not possible. Eq. (12) involves the directional derivatives, dC_i/dC_j, and these derivatives cannot be derived from the experimental data. Because of this complexity, isotherm data points cannot be derived from the determination of the retention volumes of the perturbations as functions of the two concentrations. However, knowing an iso-

therm equation, it is possible to calculate the numerical values of the coefficients of this model that best fit the experimental data.

From the equations of the isotherm model selected, the partial derivatives are derived. The coherence condition [21,23,24]

$$\frac{\mathrm{d}q_i}{\mathrm{d}c_i} = \text{const.} \quad i = 1, \ldots, n \tag{13}$$

is applied and then the directional derivatives can be calculated. For a binary isotherm, they are the solutions of the following quadratic equation:

$$\left(\frac{\mathrm{d}C_1}{\mathrm{d}C_2}\right)^2 + \frac{\mathrm{d}C_1}{\mathrm{d}C_2} \cdot \frac{\dfrac{\partial q_2}{\partial c_2} - \dfrac{\partial q_1}{\partial c_1}}{\dfrac{\partial q_2}{\partial c_1}} - \frac{\dfrac{\partial q_1}{\partial c_2}}{\dfrac{\partial q_2}{\partial c_1}} = 0 \tag{14}$$

The two roots of this equation are inserted in Eq. (12) and the retention volumes of the perturbations can now be represented as functions of the parameters of the isotherm model. The best set of numerical values of these parameters are derived using the Marquart–Levenberg iteration [25].

3. Experimental

3.1. Chemicals, solvents and columns

The feed components are the enantiomers of Tröger's base ($M_w = 250.35$ g/mol), with a structure shown in Fig. 1. The racemic mixture and small amounts of pure enantiomers were purchased from Aldrich (Milwaukee, MI, USA). The racemic mixture is only 98% pure, as determined by gas chromatography. Two purification methods were used prior to carrying out the measurements of isotherm data, recrystallization and achiral HPLC on C_{18} silica, using a 5-cm I.D. axial compression column [26]. Analytical profiles of the racemic mixtures as received and after the two different purification methods are compared in Fig. 2. Further work was carried out using the material purified by HPLC.

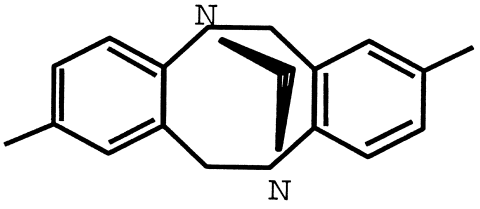

Fig. 1. Tröger's base.

These stainless steel tubes were packed with ChiralPak AD, a 20-μm particle silica-based packing material, coated with amylose tri-(3,5-dimethylphenylcarbamate) (see structure in Fig. 3). This CSP is convenient for the separation of aromatic enantiomers. The hold-up time and the total porosity of the column were measured using 1,3,5-tri-*tert.*-butyl

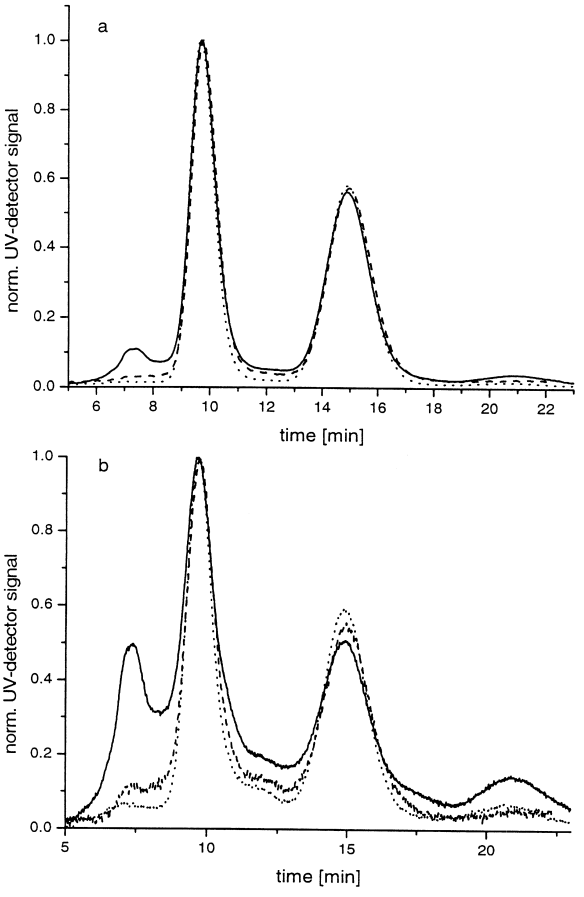

Fig. 2. Comparison of the original (Aldrich) and the purified Tröger's base racemic mixtures: Analytical injection at wavelength of 308 nm (a) and 315 nm (b) Solid line, original mixture; dashed line, mixture purified by recrystallization; dotted line, mixture purified by separation onto C_{18} silica, in a 5-cm I.D. axial compression column.

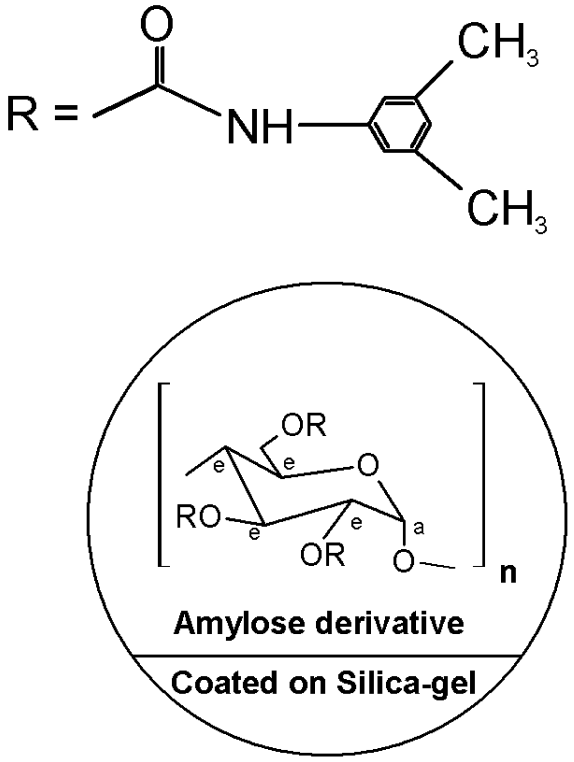

Fig. 3. Chemical structure of the CSP in Chiralpak AD [31].

benzene (TTBB) from Aldrich (Milwaukee, WI, USA). This compound is not retained but has access to the whole porosity.

HPLC-grade 2-propanol was used as the mobile phase. It was obtained from Fisher (Fair Lawn, NJ, USA) and used as received.

3.2. Analytical instrument

The column characteristics and the isotherm data were acquired using a HP 1090 liquid chromatograph (Agilent Technologies, Palo Alto, CA, USA). This instrument is equipped with a multisolvent delivery system, an automatic, programmable injection system, a high-pressure flow cell for the photodiode-array UV detector, and the HP CHEMSTATION. The cell of a laser polarimeter detector from PDR Chiral (Palm Beach, FL, USA) was located immediately downstream the cell of the UV detector. While the UV detector gives a signal that is proportional to the sum of the concentrations of the two enantiomers in the eluent, the polarimetric detector delivers a signal that is proportional to the difference between these two concentrations. Thus, after proper calibration of the two detectors, it is easy to derive the concentration profiles of the two enantiomers in the column eluent. The experimental data of the polarimeter were acquired using an A/D converter HP 35900E from Agilent or a data acquisition system from LabView (National Instruments, Austin, TX, USA).

3.3. Procedures

3.3.1. Frontal analysis

The UV detector was calibrated at a wavelength of 308 nm, at which UV absorption by the product impurities is small and the deviation from linear behavior of the detector response in the range of concentrations investigated is moderate. The response of the polarimeter was found to be linear in this same range. The hold-up volume of TTBB was measured and corrected for the dead volume contribution of the liquid chromatograph, by replacing the column with a zero-volume connector. This allowed the derivation of the column porosity and its phase ratio (see Table 1).

An analytical size injection of the racemic mixture of Tröger's base provided the retention volumes that are used to calculate the Henry coefficients a_i of the two enantiomers as well as their separation factor (Table 1).

The acquisition of FA data was carried out using the solvent delivery system of the liquid chromatograph to provide single step injection of the two enantiomers in the mobile phase [27]. Pure mobile phase being solvent A and feed sample being solvent

Table 1
Analytical column parameters

1,3,5-Tri-*tert*.-butyl benzene		
Retention volume, V_0 (ml)		5.144
Porosity, ε		0.648
Phase ratio, F		0.543
Number of theoretical plates, N_{TTBB}		1270
Tröger's base	+	−
Retention volume V_r (ml)	9.835	14.717
Henry coefficient, a	1.679	3.426
Number of theoretical plates, N	560	420

B, ten successive step increases of 10% of the concentration of B in A were programmed. The flow-rate was 1 ml/min and the injection time was 40 min. The column was regenerated after the each step by flushing away the feed with a stream of pure mobile phase. This procedure was successively applied to feeds containing each enantiomer (5.52 or 5.23 g/l of the pure (+)- or (−)-enantiomers, respectively) and the racemic mixture (total concentration of 10, 20 and 14.96 g/l). The experiments at the concentration of 14.96 g/l carried out at a flow-rate of 0.5 l/min and a step period of 80 min. The breakthrough curves at the concentration of 10 g/l were recorded by the combination of the UV and the polarimetric detectors. The composition of the intermediate plateau was derived from the appropriate combination of the two signals.

3.3.2. Perturbation method

Once the plateau concentration of the eluent in the FA method is recorded, signaling that equilibrium has been reached between the mobile and the stationary phase, a perturbation of this equilibrium is made by injecting a 20-μl sample of the solvent. No calibration was needed to account for the data but the retention volumes are corrected for the hold-up contribution of the liquid chromatograph (see earlier). These experiments were performed at a flow-rate of 1 ml/min. Because pure mobile phase is injected as the perturbation, all perturbation peaks were negative.

3.4. Overloaded concentration profiles

Due to the limited solubility of Tröger's base in 2-propanol, concentration profiles under nonlinear conditions were produced by a combination of concentration and volume overload. Single-step pulse injections were performed with the help of two pumps, where pump A and B delivered the solvent and sample, respectively. This procedure also reduced band broadening caused by axial dispersion in the injection loop. The amount injected was varied by changing the injection time and the composition of the injected sample. The type of overload had to be considered when the experimental and simulated concentration profiles were compared.

4. Results and discussion

The column characteristics and the analytical parameters of the Tröger's base enantiomers in the chromatographic system were determined before the acquisition of the experimental data characterizing their adsorption behavior. The values of these parameters are reported in Table 1. The column used has the relative high efficiency of 1270 plates determined from analytical injection of TTBB. The total column porosity, $\epsilon = 0.648$, was derived from the retention volume of this non-retained compound. The Henry coefficients of the two enantiomers were derived from their retention volumes at infinite dilution. These coefficients give the initial slopes of the isotherms, an important feature. The separation factor of 2.04 indicates an easy separation. For the less and more-retained enantiomers the numbers of theoretical plates were estimated to be 560 and 420 plates, respectively.

4.1. Parameter estimation for adsorption isotherm models

4.1.1. Experimental results of frontal analysis

Frontal analysis as described in Sections 2.3.1 and 3.3.1 was applied initially in an attempt to find the adsorption isotherm model to which the experimental data would fit best. Due to the unique adsorption behavior of Tröger's base on the CSP, several models were examined. The best numerical values of their parameters are listed in Table 2. The nonlinear curve fitter of the ORIGIN software package (Microcal Software) was used to perform the parameter estimation. Each isotherm parameter in the table is shown with the corresponding estimate of the standard error [28]:

$$\sigma_i = \sqrt{C_{ii}\chi^2} \tag{15}$$

where C_{ii} is the diagonal element of the variance–covariance matrix $C = (\boldsymbol{F}' \otimes \boldsymbol{F})^{-1}$. $\boldsymbol{F}$ is the Jacobian $\boldsymbol{F}_{i,j} = \partial f(x_{1i}, x_{2i}, \ldots; p_1, p_2, \ldots)/\partial p$ where f, x, and p are the fitting function, the independent variables, and the parameters of the fitting function, respectively.

Table 2
Adsorption isotherm parameters determined by frontal analysis

Model	q_s (g/l)	b_1 (l/g)	b_2 (l/g)	b_{12} (l/g)	b_{22} (l^2/g^2)	R^2	χ^2
(+) Tb best fit Langmuir Eq. (6)	58.167	0.02796				0.9999	0.00043
(+) Tb Langmuir Eq. (6)	58	0.02894				0.9969	0.01775
(−) Tb best fit quadratic Eq. (8)	17.954		0.1179		0.05414	0.9991	0.06434
(−) Tb quadratic Eq. (8)	25		0.1298		0.02335	0.9977	0.12503
rac Tb non-comp. Langmuir Eq. (6)	335.8	0.0051				0.9951	0.1515
rac Tb non-comp. quadratic Eq. (8)	25		0.1298		0.02289	0.9993	0.08995
rac Tb best fit comp. Langmuir Eq. (6)	192.8895	0.01071	0.02332			0.99349	0.7127
rac Tb comp. Langmuir Eq. (6)	193	0.0087	0.01682			0.85659	14.82604
rac Tb best fit comp. quadratic Eqs. (7)–(8)	45.73	0.01619	0.08335	0.00983	0.00237	0.9982	0.22456
rac Tb comp. quadratic Eqs. (7)–(8)	45.73	0.03672	0.07098	0.00735	0.00474	0.9934	0.68504
purified *rac* Tb Langmuir Eq. (6)	335.8	0.00483				0.9994	0.00941
purified *rac* Tb quadratic Eq. (8)	25		0.1298		0.02191	0.9991	0.0717
purified *rac* Tb best fit comp. quadratic Eqs. (7)–(8)	33.957	0.02661	0.09051	0.0159	0.00885	0.9991	0.06972
purified *rac* Tb comp. quadratic Eqs. (7)–(8)	33.3	0.05022	0.0975	0.01355	0.01181	0.9973	0.1833

The correlation coefficient R^2 has a value between zero and one, with one representing a perfect fitting. The coefficient is calculated with the following relationship:

$$R^2 = 1 - \frac{\Sigma w_i [y_i - f_i]^2}{\Sigma w_i \left[y_i - \frac{\Sigma w_i y_i}{\Sigma w_i} \right]} \tag{16}$$

where w_i describes the weighting function. The reciprocal of the square of the data set, y^{-2}, was chosen as the weighting function. In addition, the software calculates the value of χ^2, a parameter that has an inverse relationship to the goodness of the fit with the experimental data set. For multiple fitting functions the value of this parameter is determined as:

$$\chi^2(p_1, p_2 \ldots) = \frac{1}{n-p} \Sigma_i \Sigma_j w_{i,j} [y_i - f(x_{1i}, x_{2i}, \ldots; p_1, p_2, \ldots)]^2 \tag{17}$$

where n represents the total number of experimental data points.

The whole set of data points obtained by FA in a series of measurements discussed below is shown in Fig. 4. These results include those derived from measurements made with the initial racemic mixture, with the racemic mixture purified by preparative HPLC, and with samples of the two pure enantiomers, as well as data derived from particular processing of the signal of the polarimetric detector. These particular results are discussed in more detail now.

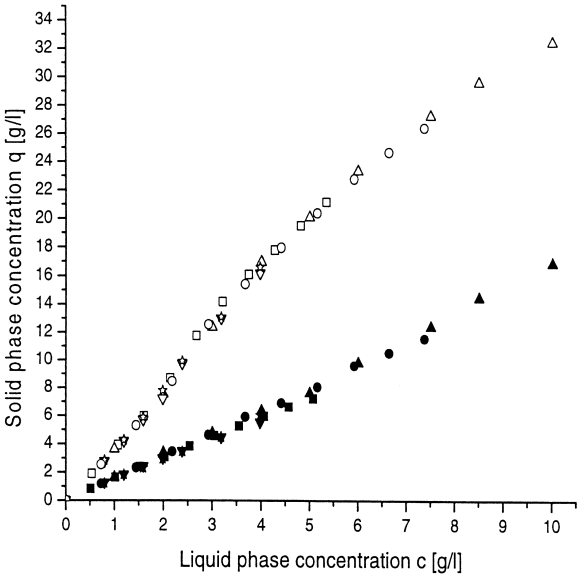

Fig. 4. Whole set of experimental adsorption isotherm data determined by frontal analysis. Solid symbols, less-retained enantiomer; open symbols, more-retained enantiomer; square symbols, measurements made with the pure enantiomer; triangles upward, measurements made with the racemic mixture and $C_t = 20$ g/l; triangles downward, measurements made with the racemic mixture and $C_t = 7.96$ g/l; stars, values derived from the combination of the signals of the UV and polarimetric detectors and $C_t = 7.96$ g/l; circles, values derived from the sole polarimetric detector signal and $C_t = 14.5$ g/l.

As explained previously, the initial experiments were performed using the original raw racemic mixture purchased from Aldrich with the total concentration of 20 g/l. Due to the unusual adsorption behavior of the two enantiomers and to the presence of important impurities (see Fig. 2), the concentration profiles of the experimental breakthrough curves of the racemic mixture exhibited no clear fronts nor intermediate plateaus, as those usually observed [2,20,27]. The fact that the height of the intermediate plateau was lower than half of the total concentration was particularly unusual and required explanations that could not be obtained easily from the analysis of the FA data (see later). Nevertheless, these experimental data were used to determine the adsorption isotherm points, following the classical integral mass balance equation [20]:

$$q_x = \frac{C_x(V_{1+2} - V_0) - C_{x,ip}(V_{1+2} - V_1)}{V_s} \quad (18)$$

where V_0, V_1, V_{1+2}, and V_s are the hold-up volume of the column, the retention volume of the first and second adsorption fronts, and the volume of the stationary phase, respectively. The variable x indicates the compound. The results obtained in these experiments are shown as upward triangles in Fig. 4.

To improve the accuracy of the experimental FA data, the original racemic mixture was purified by two different methods: recrystallization and preparative chromatography. The cleaned mixture samples are compared to the original sample in Fig. 2. However, the impurities could not be entirely eliminated. Although at their low concentrations these remaining impurities do not influence significantly the adsorption behavior of the enantiomers studied, their presence affects the accuracy of the UV detector calibration, an effect that is more serious for the breakthrough profiles of FA than for the peaks of PM. The adsorption isotherms were determined again by both methods. The total concentration of the feed solution was 14.5 g/l. The experimental data are displayed in Fig. 4 as downward triangles.

Frontal analysis measurements were also performed for the single compounds. Due to the limited amount of pure enantiomers available, these measurements were carried out using only one solution B for each enantiomer. The concentrations of these solutions were 5.52 and 5.233 g/l for the less- and the more-retained compounds, respectively. The data are shown in Fig. 4 (squares).

In the cases of disperse breakthrough curves, impurities influencing the UV detector response, and/or small separation factors α, the determination of the intermediate plateau concentration is very difficult if not impossible. It would be useful if the breakthrough of the two enantiomers could be resolved. The proper combination of the responses of the UV and the polarimetric detector allows this, so a further series of FA measurements was carried out with both these detectors on-line. The single concentration breakthrough profiles were calculated following the method explained in detail in [29]. The data points obtained by this method are shown in Fig. 4 as stars. Data derived from the single polarimetric detector signal are shown as circles. Because the polarimeter gives no response to nonchiral impurities, their presence should not affect the detector signal as they do that of the UV detector. A more detailed comparison of the experimental iso-

therm data points determined either from the sole signal of the polarimeter (○) or from the combination of the signals of the UV detector and the polarimeter (◇) shows only small deviations between the two sets of data. The notable ones are at high concentrations and around the inflection point of the isotherm of the more-retained enantiomer.

To verify the reliability of our measurements isotherm data points were calculated from both sides of the FA breakthrough curves. The following classical equation was used for calculating the rear front data points:

$$q_x = \frac{C_x(V_{1+2} - V_0) + C_{x,ip}(V_{1+2} - V_2)}{V_s} \quad (19)$$

where V_{1+2} and V_1 are the retention volumes of the first and second desorption fronts, respectively. The data sets (not shown) are identical for the less-retained enantiomer. Only in the high concentrations range could a small difference be observed for the more-retained enantiomer.

To return to Fig. 4 in which all the experimental data determined by FA are shown, we observe that, although samples of the racemic mixture of different degrees of purity and samples of the pure enantiomers were used, no significant differences between the different sets of data points can be found and the scatter of the whole points is small in spite of the different origins of these data. The data obtained for the more-retained enantiomer suggest a noncompetitive behavior with the less-retained one. By contrast, an atypical behavior was observed for the less-retained enantiomer. The whole set of data does not fit well to the Langmuir model; when the data obtained with the pure enantiomer are fitted separately, the binding capacity is lower than the one derived from a fit of the data for the racemic mixture. This does not suggest a competitive but rather a cooperative behavior.

At this point it would be reasonable to conclude the parameter estimation for this chiral separation system and describe it with noncompetitive Langmuir and quadratic isotherm models for the less and more-retained compounds, respectively. However, allowing to remaining uncertainties about the reliability of the experimental data sets as well as the observation of a rather unique adsorption behavior of the less-retained compound additional investigations were proposed.

4.1.2. Experimental results of the perturbation method (PM)

As described in more detail in Sections 2.3.2 and 3.3.2 the perturbation method has one main advantage over FA. It does not require an exact calibration of the UV detector and it gives data that are not affected by the sample impurities. Analytical peaks are recorded and their retention volumes measured. The concentration dependence of these retention volumes characterizes the adsorption behavior and permits the selection of the best isotherm model and the determination of the numerical values of its parameters. We followed the steps described in Blümel et al. [7]. The parameters of the chosen isotherm model are estimated by minimizing the objective function OF (Eq. (8) [7]):

$$\mathrm{OF}_{\bar{V},\bar{c}} = \sum_{m=1}^{M} \sum_{k=1}^{N} \left(\frac{[V^m_{\mathrm{r,k,ex}} - V^m_{\mathrm{r,k,th}}(\bar{c}^m_{\mathrm{ex}})]}{V^m_{\mathrm{r,k,ex}}} \right)^2 \quad (20)$$

with a nonlinear regression algorithm from Marquardt–Levenberg [25]. In Eq. (20) the variables m and k are the number of experimental data points and of components, respectively. The retention volume predicted by the model, $V^m_{\mathrm{r,k,th}}$, is calculated from Eq. (11) (see Section 2.3.2). To evaluate the goodness of the fitting functions the sum of the least square errors SLQ [Eq. (21)] and the standard deviation SD [Eq. (22)] are computed:

$$\mathrm{SQ} = \sum_i [x_i - \hat{x}]^2 \quad (21)$$

$$\mathrm{SD} = \sqrt{\frac{1}{n-p} \sum_i [x_i - \hat{x}]^2} \quad (22)$$

where x_i, $\hat{x}$, n, and p are the measured and calculated data sets, the number of experimental data points and the number of parameters, respectively. These parameters are inversely related to the quality of the fit. In Table 3 the best estimates of the isotherm parameters are listed as well as the corresponding statistical values. The experimental results are reported in Fig. 5. The difference between the behavior of the data obtained for the two enantiomers is striking. There seems to be little difference between the retention times of the perturbations corresponding to the more-retained enantiomer and obtained with either the pure compound or the racemic mixture. This confirms the lack of competition by the

Table 3
Adsorption isotherm parameters determined by the perturbation method

Model	q_s (g/l)	K_1 (l/g)	K_2 (l/g)	K_{d1} (l/g)	K_{d2} (g/l)	K_{21} (l/g)	K_{d21} (l/g)	SD	SLQ
Three-layer Eq. (9)	28.25	0.05946	0.1212	0.009225	0.1147	0.02216	0.3097	0.2582	2.867
	$q_{max}b_a$	b_a (l/g)	b_b (l/g)	K_2 (l/g)	q_s (g/l)	b_2 (l/g)	b_{22} (l^2/g^2)		
Coop-quadratic Eq. (10)	1.679	0.0311	−0.03862	−0.7319	27	0.1269	0.01532	0.6175	40.04
	q_s (g/l)	b_1 (l/g)	b_2 (l/g)	b_{12} (l/g)	b_{22} (l^2/g^2)				
Comp-quadratic Eqs. (7) and (8)	54	0.0311	0.0634	0.010795	0.0068			0.6126	40.164
Best fit comp-Langmuir Eq. (6)	313.961	0.0004783	0.012136					0.6075	40.22
Comp-Langmuir Eq. (6)	54	0.0311	0.0635					0.6	41.951

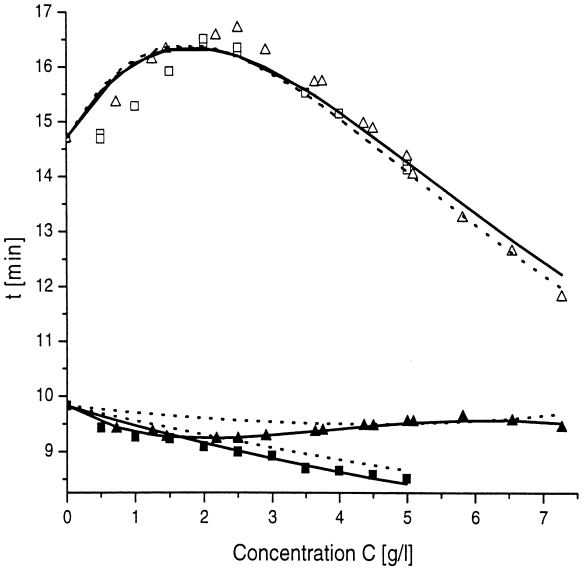

Fig. 5. Retention times of the perturbations versus the concentration of the plateaus. Symbols: experimental data; solid symbols, less-retained enantiomer; open symbols, more-retained enantiomer; squares, values obtained for pure enantiomers; triangles, values obtained with the racemic mixture. Lines: best fit of the isotherm models to the data; dashed line, cooperative-quadratic isotherm models Eq. (10); solid line, three-layer isotherm model Eq. (9).

less-retained enantiomer in the adsorption of the more-retained one. On the other hand, the presence of the more-retained enantiomer and its concentration affect considerably the adsorption of the less-retained one. The effect is unexpected as it shows a cooperative adsorption behavior, not a competitive one.

4.1.3. Determination of the isotherm model

The experimental data determined by PM were first fitted to the competitive Langmuir isotherm model. The fitting was performed with two different assumptions. First, the initial slope of each isotherm (i.e. the Henry coefficient a_i) was kept floating. Second, it was set equal to the value derived from the retention factors measured at infinite dilution. The best estimates of the isotherm parameters obtained are listed under names bestfitcomp.Langmuir and comp.Langmuir in Table 3. The free-parameter estimation gave slightly better statistical results but neither of them could describe the behavior of the retention volumes (times) in Fig. 5. Both profiles in Fig. 5 exhibit very unique behavior, both in agreement with the data in Fig. 4. The isotherm of the more-retained enantiomer does have an inflection point and exhibits no influence of the concentration of the less-retained enantiomer. The isotherm measured for the pure less-retained enantiomer behaves

as a classical Langmuir isotherm. The retention time of the corresponding perturbation decreases with increasing concentration of the compound. However, in a mixture with the other enantiomer, the behavior becomes very unusual. The less-retained enantiomer is adsorbed more strongly to the stationary phase than as a pure compound. The classical displacement effect cannot be observed. For the sake of completness, the fitting was also performed for the competitive quadradic model. A good agreement could be reach, however, the model did not describe the shape of the isotherm curve of the less-retained enantiomer at all.

The experimental data were then fitted to the cooperative-quadratic isotherm. The best values of the isotherm parameters are displayed in Table 3 and compared to the experimental data in Fig. 5 (dotted line). For the sake of simplification we assumed that there was no influence of the less-retained enantiomer on the adsorption behavior of the more-retained one. The agreement between this isotherm model and the experimental data are much better than the one that could be obtained with any other combination of single component or binary isotherms. However, the behavior of the less-retained compound when in the racemic mixture is not described sufficiently well.

As a last step, we fitted the data to the multilayer isotherm model (Eqs. 8 and 10). The corresponding parameters are also listed in Table 3. The comparison between the experimental data and the fitting in Fig. 5 shows an excellent agreement, especially for the less-retained enantiomer. Only one of the third-layer parameters of this model, K_{d211}, proved to be significant. In an extended study [19], this unique adsorption behavior of Tröger's base is explained with the help of molecular modeling tools. The microscopic findings support our macroscopic results. Due to the insignificance of the parameter K_{d12} the model is reduced to a seven-parameter model. Finally, the experimental data measured by frontal analysis are compared in Fig. 6 to the two best adsorption isotherm models determined from the perturbation method experiments and discussed above, the cooperative-quadratic isotherm and the multilayer isotherm models. For the more-retained enantiomer the FA data and the two adsorption isotherm models agree very well. There is a significant deviation between the experimental data and the

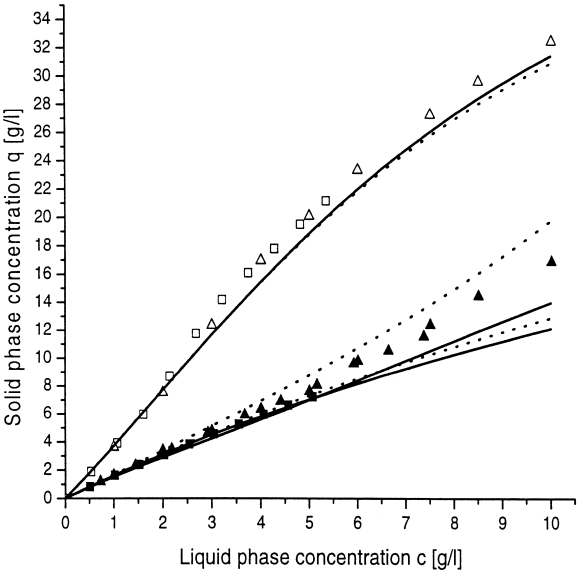

Fig. 6. Comparison between fitting models determined by PT and experimental results measured by frontal analysis: solid symbols, less-retained compound; open symbols, more-retained compound; square, single enantiomer measurements; triangle, racemic mixture measurements; dashed line, cooperative-quadratic isotherm fitting function Eq. (10), and solid line, three-layer isotherm fitting function Eq. (9).

predictions of the two models for the less-retained enantiomer. Although the experimental data obtained with the racemic mixture (middle lines) and with the three-layer isotherm model exhibit both a concave-upward tendency, the degree of this curvature is slightly different. The slope of the cooperative-quadratic model (dotted line) increases more rapidly than that of the three-layer isotherm (solid line).

An additional remark concerning the unique adsorption behavior of Tröger's base onto the CSP on the results of enantiomerization tests [30] should be made. Both pure enantiomers dissolved in 2-propanol were separately stored in presence of the stationary phase for 2 weeks at room temperature. Comparing the initial with the final analytical elution profiles reveals no difference in the composition of the samples. Neither sample shows any enantiomerization effects under the operating condition, therefore, we can rule out this effect as a cause for the unique adsorption behavior of Tröger's base. The pure enantiomers kept their stereointegrity.

4.2. Comparison of experimental and simulated concentration profiles

The results of isotherm modeling should be validated by comparing the experimental and calculated band profiles in overloaded elution and SMB chromatography. The calculations were performed by numerically solving the mass balance Eq. (1) using the backward–forward FD algorithm previously described [2,10]. For the sake of simplification, only the cooperative quadratic isotherm and the multilayer isotherm models were used.

High concentration experimental breakthrough profiles (solid lines) obtained in FA and those calculated using the two isotherm models are compared in Figs. 7 and 8. The experimental profiles were recorded by the UV detector and the polarimeter. Therefore, not only the concentration profiles of the racemic mixture but also the profiles of the two pure enantiomers are available for the comparison. All calculations were performed with a column efficiency of 250 theoretical plates. The adjustment of the theoretical plate number was necessary to account for dispersion and mass transfer effects

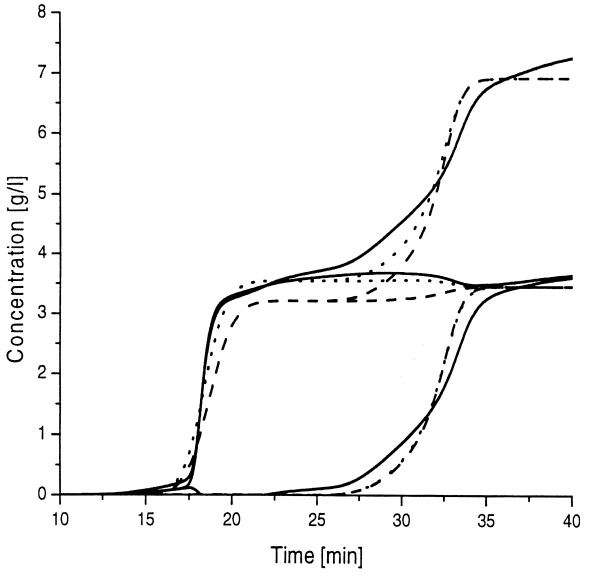

Fig. 7. Comparison between fitting models determined by PT and experimental frontal profiles: $C_t = 7.96$ g/l and 0.5 ml/min, solid line, experimental data; dotted line, simulation with three-layer isotherm model Eq. (9); dashed line, simulation with cooperative-quadratic isotherm model Eq. (10).

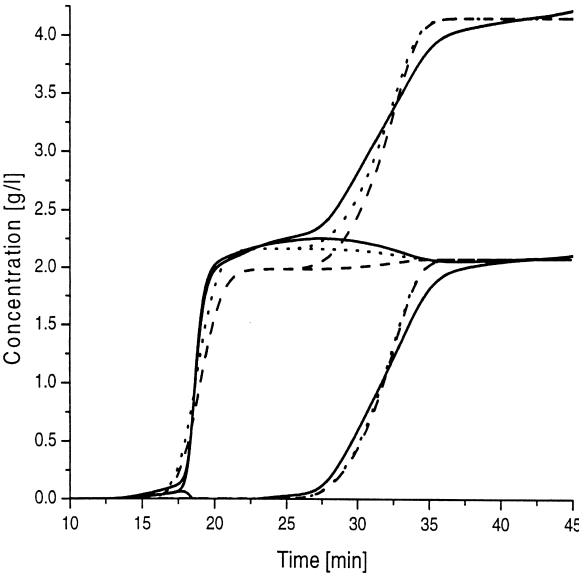

Fig. 8. Comparison between fitting models determined by PT and experimental frontal profiles: 60% $C_t = 7.96$ g/l and 0.5 ml/min, solid line, experimental data; dotted line, simulation with three-layer isotherm model Eq. (9); dashed line, simulation with cooperative-quadratic isotherm model Eq. (10).

under these overloaded conditions. The dashed and dotted lines represent the results of the cooperative quadratic and of the three-layer isotherm models, respectively. As expected, both models describe the shape of the more-retained compound quite well. However, the front of the cooperative-quadratic model is more disperse than the experimental front and the front simulated by the three-layer model (the latter agrees so well with experimental data that it cannot be distinguished in most places). Different heights of the intermediate plateaus can also be observed. The cooperative-quadratic model predicts a concentration lower than half of the total mixture concentration. Although the concentration profiles detected by UV detector also indicate such a behavior for all intermediate plateaus of the mixture, the combination of both detectors showed that the heights of these intermediate plateaus are indeed higher and that they decrease with increasing concentration. Most of these discrepancies are explained by inaccuracies in the estimation of the experimental concentration profiles.

Because the Tröger's base samples contain signifi-

cant concentrations of UV-absorbing impurities that are not chiral, the UV detector signal is, at some times, larger than what corresponds to the sum of the concentrations of the two enantiomers while the polarimeter signal corresponds always to the difference between the concentrations of the two enantiomers. During calibration, the impurities are all present and the signal is overestimated. During the chromatographic measurements, all the impurities are not simultaneously present; they are mostly eluted before the main peak. The error on the concentration profiles of the two enantiomers is estimated to be of the order of a few percents. To minimize it, band profile comparisons were made for large size samples obtained with solutions of only 6.9 g/l. This permitted the achievement of a better agreement between calculated and the experimental data. With this adjustment the three-layer model describes the experimental fronts very well.

Overload elution experiments were performed with the pure enantiomers and with samples of the racemic mixture. These concentration profiles are compared to those calculated using the two proposed models. In Figs. 9, 10, and 11 the experimental results and the predictions of the cooperative-quadratic and the three-layer models are reported as the solid, the dashed, and the dotted lines, respectively. Fig. 9 shows the volume overload profiles of the less-retained enantiomer. The calculations were performed with a column efficiency of 700 theoretical plates. At the largest injection of 2 ml the top concentration plateau is almost formed. The profiles calculated by the cooperative-quadratic model elutes slightly later than the experimental profiles and those calculated with the three-layer model slightly earlier. However, both models describe the single compound profiles very well. The calculations of the concentration overload of the second compound give very similar results for both models (see Fig. 10). The profiles calculated with either model are eluted earlier than the experimental profiles. The largest difference in retention times takes place for concentrations close to that of the inflection point of the isotherm. Nevertheless, the calculated profiles have the same shapes as the experimental profiles. Finally, the overloaded experimental profiles of the racemic mixture are compared to the calculated profiles in Fig. 11. Similar conclusions can be drawn as for the

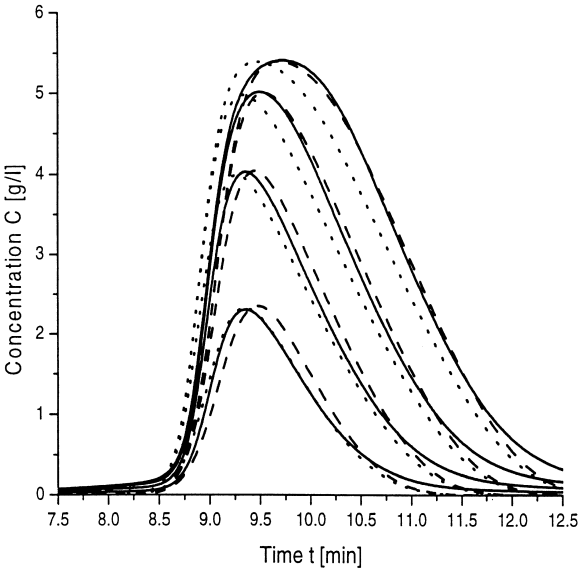

Fig. 9. Comparison between fitting models determined by PT and experimental overload profiles of the less-retained enantiomer: 0.5, 1, 1.5 and 2 min injection of $C_t = 5.52$ g/l and 1 ml/min, solid line, experimental data; dotted line, simulation with three-layer isotherm model Eq. (9); dashed line, simulation with Langmuir isotherm model Eq. (6).

single compound profiles. The two models gave an excellent agreement with the experimental profiles for the more-retained compound; these profiles are almost indistinguishable. The largest difference in the retention times with the experimental values takes place also near the inflection point of the isotherms. For the less-retained compound, the experimental profiles and those calculated with the cooperative-quadratic model are nearly identical. The profiles calculated with the three-layer isotherm elute slightly faster than the experimental profiles.

5. Conclusions

There are two important issues of practical and fundamental importance in this study. First, the presence of impurities in the available sample of racemic mixture of Tröger's base, in spite of partly successful attempts at purification, affects the response of the UV detector. This could also have affected the adsorption behavior of the racemic

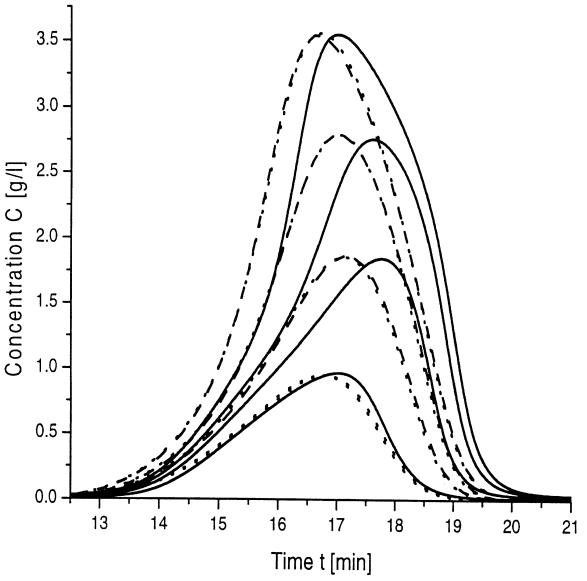

Fig. 10. Comparison between fitting models determined by PT and experimental overload profiles of the more-retained enantiomer: 25, 50, 75 and 100% of $C_t = 5.233$ g/l and 1 ml/min, solid line, experimental data; dotted line, simulation with three-layer isotherm model Eq. (9); dashed line, simulation with quadratic isotherm model Eq. (8).

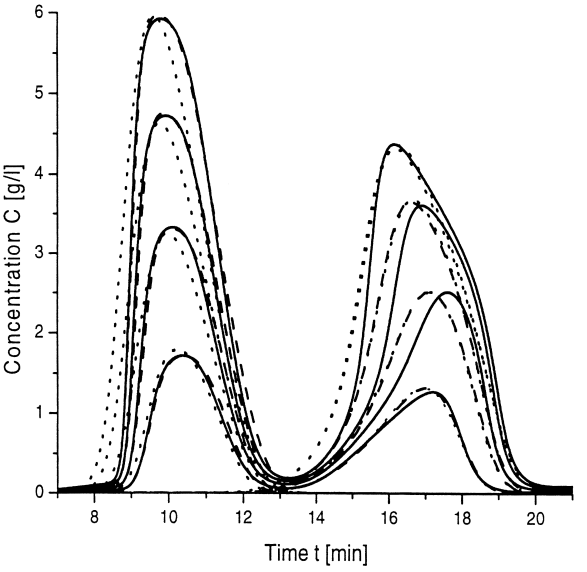

Fig. 11. Comparison between fitting models determined by PT and experimental overload profiles of the racemic mixture: 25, 50, 75 and 100% of $C_t = 14.5$ g/l and 1 ml/min; solid line, experimental data; dotted line, simulation with three-layer isotherm model Eq. (9); dashed line, simulation with cooperative-quadratic isotherm model Eq. (10).

mixture but it did not. The results of this work prove that alternative methods to the classical FA method help in acquiring data and validating the FA data. The combination of the UV detector and the polarimeter reduces the influence of the impurities on the profiles. If the impurities have no chiral properties, as in our case, using only the signal of the polarimeter can permit the acquisition of accurate FA data. The accuracy of this measurements was demonstrated. Using both the adsorption and the desorption front for the FA determination of adsorption isotherm data is recommended, at least for the sake of data validation, especially for systems with disperse fronts, mixtures with vanishing intermediate plateaus, or isotherms with inflection points. The perturbation method has several advantages over FA. Not only is there no calibration of the UV detector required, but also the perturbation peaks are still detectable when the intermediate plateau has already vanished. The behavior of the retention volumes (or the retention times) indicates clearly how the adsorption of the compounds onto the stationary phase occurs. However, the fitting procedure becomes more complicated with more complex isotherm models, due to use of the total derivatives of the adsorption isotherm. Second, the adsorption of Tröger's base revealed a most unusual behavior. The isotherm of the more-retained enantiomer has an inflection. Furthermore, there is an unusual cooperative adsorption behavior of the more-retained enantiomer on the less-retained one. The saturation capacity of this less-retained enantiomer increases with the concentration of the other enantiomer. The unique adsorption behavior of Tröger's base lead us to use a relatively sophisticated isotherm model but thermodynamics easily provided the required tool. This is important because a correct isotherm model is the basis for any other work in the field of preparative chromatography, especially for finding the optimal operating conditions of SMB applications. In another report [29] we showed the great usefulness of the model discussed here in predicting accurate band

profiles along the SMB and production rates in agreement with experimental data.

Finally, we hope to have answered the remaining questions from the previous work [9] concerning the adsorption behavior of Tröger's base onto a similar CSP with the results provided in this study.

6. Notation

a_i	Henry isotherm coefficient
b_a	isotherm parameter
b_b	isotherm parameter
b_i	isotherm parameter (cm^3/g)
b_{ij}	isotherm parameter Eqs. (7) and (8) (cm^3/g)
b_{ii}	isotherm parameter Eqs. (7) and (8) (cm^3/g)
C	liquid phase concentration (g/cm^3)
C_{ii}	diagonal element of the variance–covariance matrix $\boldsymbol{C}$
D_{ap}	axial dispersion coefficient (cm^2/s)
F	phase ratio
$\boldsymbol{F}$	Jacobian of the fitting function f
f	fitting function
K_i	equilibrium constant Eq. (9)
K_{di}	equilibrium constant Eq. (9)
K_{dij}	equilibrium constant Eq. (9)
K_{djii}	equilibrium constant Eq. (9)
k_2	isotherm parameter Eq. (9)
L_C	column length (cm)
N	theoretical number of plates
n	number of experimental points
OF	objective function
p	number of parameters
q	solid-phase concentration (g/cm^3)
q_{max}	maximal saturation capacity (g/cm^3)
q_s	saturation capacity (g/cm^3)
SD	standard deviation
SLQ	sum of least square error
t	time (s)
u	liquid phase flow velocity (cm/s)
V	volume (cm^3)
w_i	weighting function
$\dot{V}$	volumetric flow-rate (ml/min)
x	independent variable
y	dependent variable
z	axial coordinate

Greek symbols

α	separation factor
ϵ	overall void fraction
σ	standard error
χ	nonlinear regression function

Subscripts

0	nonretained compound
ex	experimental
feed	feed
i	component ($i=1, 2$)
ini	initial
l	liquid
p	pulse
s	solid
r	retention
th	theoretical

Acknowledgements

This work was supported in part by Grant CHE-00-70548 of the National Science Foundation and by the cooperative agreement between the University of Tennessee and the Oak Ridge National Laboratory. Additional funding was given by NATO grant (OUTR.LG971480). The authors are grateful to Chiral Technologies, for the supply of the packing material Chiralpak AD and sample of the single enantiomers, and to G. Yanik from PDR Chiral, for his continuous technical support.

References

[1] FDA, Chirality 4 (1992) 338.
[2] G. Guiochon, S.G. Shirazi, A.M. Katti, Fundamentals of Nonlinear and Preparative Chromatography, Academic Press, Boston, MA, 1994.
[3] R.-M. Nicoud, A. Seidel-Morgenstern, Isolation and Purification 2 (1996) 165.
[4] A. Seidel-Morgenstern, Deutscher Universitätsverlag, Wiesbaden (1995).
[5] E. Glueckauf, J. Chem. Soc. (1947) 1302.

[6] A. Seidel-Morgenstern, C. Blümel, H. Kniep, in: F. Meunier (Ed.), Fundamentals of Adsorption 6, Elsevier, Amsterdam, 1998, p. 303.
[7] C. Blümel, P. Hugo, A. Seidel-Morgenstern, J. Chromatogr. A 827 (1998) 175.
[8] B.J. Stanley, C.R. Foster, G. Guiochon, J. Chromatogr. A 761 (1996) 41.
[9] A. Seidel-Morgerstern, G. Guiochon, J. Chromatogr. 631 (1993) 37.
[10] P. Rouchon, M. Schonauer, P. Vaentin, G. Guiochon, Sep. Sci. Technol. 22 (1987) 1793.
[11] K.O. Friedrichs, R. Courant, H. Lewy, Math. Ann. 100 (1928) 32.
[12] K. Kaczmarski, D. Antos, J. Chromatogr. A 756 (1996) 73.
[13] K. Kaczmarski, D. Antos, Comput. Chem. Eng. 20 (1996) 1271.
[14] T.L. Hill, An Introduction to Statistical Thermodynamics, Addison-Welsley, Reading, MA, 1960.
[15] B. Lin, Z. Ma, S. Golshan-Shirazi, G. Guiochon, J. Chromatogr. 475 (1989) 1.
[16] D.M. Ruthven, M. Goddard, Zeolites 6 (1986) 276.
[17] M. Diack, G. Guiochon, Anal. Chem. 63 (1991) 2608.
[18] K. Mihlbachler, B. Anspach, A. Seidel-Morgenstern, Chem.-Ing. Techn. 70 (1998) 382.
[19] K. Mihlbachler, M. DeJesus, M.J. Sepaniak, K. Kaczmarski, A. Seidel-Morgenstern, G. Guiochon, in preparation.
[20] J. Jacobson, J.H. Frenz, Cs. Horvath, Indust. Eng. Chem. Res. 26 (1987) 43.
[21] F.G. Helferich, G. Klein, Multicomponent Chromatography, Marcel Dekker, New York, 1970.
[22] H. Kabir, G. Grevillot, D. Tondeur, Chem. Eng. Sci. 53 (1998) 1639.
[23] H. Rhee, R. Aris, N.R. Amundson, in: First Order Partial Differential Equations, Vol. I, Prentice-Hall, Englewood Cliffs, NJ, 1986.
[24] H. Rhee, R. Aris, N.R. Amundson, in: First Order Partial Differential Equations, Vol. II, Prentice-Hall, Englewood Cliffs, NJ, 1986.
[25] D.W. Marquardt, J. Soc. Appl. Math. 11 (1963) 431.
[26] K. Mihlbachler, Dissertation (in preparation).
[27] S. Khattabi, D.E. Cherrak, J. Fischer, P. Jandera, G. Guiochon, J. Chromatogr. A 877 (2000) 95.
[28] Inc. Microcal Software, (1999)
[29] K. Mihlbachler, A. Jupke, A. Seidel-Morgenstern, H. Schmidt-Traub, G. Guiochon, J. Chromatogr. A 944 (2002) 3.
[30] O. Trapp, V. Schurig, J. Am. Chem. Soc. 122 (2000) 1424.
[31] www.chiraltechnologies.com, Dec. 12 (2000).